FULL PAPER

Dalton
www.rsc.org/dalton

Reactions of Li- and Yb-coordinated *N*,*N*′-bis(trimethylsilyl)-β-diketiminates: one- and two-electron reductions, deprotonation, and C–N bond cleavage

Anthony G. Avent, Peter B. Hitchcock, Alexei V. Khvostov, Michael F. Lappert* and Andrey V. Protchenko

The Chemistry Laboratory, University of Sussex, Brighton, UK BN1 9QJ.
E-mail: m.f.lappert@sussex.ac.uk; Fax: +44 1273 677196; Tel: +44 1273 678316

Received 14th April 2004, Accepted 26th May 2004
First published as an Advance Article on the web 18th June 2004

The synthesis and characterisation of novel Li and Yb complexes is reported, in which the monoanionic β-diketiminato ligand has been (i) reduced (SET or 2 × SET), (ii) deprotonated, or (iii) C–N bond-cleaved. Reduction of the lithium β-diketiminate Li($L^{R,R'}$) [$L^{R,R'}$ = N($SiMe_3$)C(R)CHC(R′)N($SiMe_3$)] with Li metal gave the dilithium derivative [Li(tmen)(μ-$L^{R,R'}$)Li(OEt_2)] (**4**, R = R′ = Ph; or **5**, R = Ph, R′ = Bu^t). When excess of Li was used the dimeric trilithium β-diketiminate [$Li_3(L^{R,R'})$(tmen)]$_2$ (**6**, R = R′ = C_6H_4Bu^t-4 = Ar) was obtained. Similar reduction of [Yb($L^{R,R'}$)$_2$Cl] gave [Yb{(μ-$L^{R,R'}$)Li(thf)}$_2$] (**1**, R = R′ = Ph; or **2**, R = R′ = C_6H_4Ph-4 = Dph). Use of the Yb–naphthalene complex instead of Li in the reaction with [Yb($L^{Ph,Ph}$)$_2$] led to the polynuclear Yb clusters [$Yb_3(L^{Ph,Ph})_3$(thf)] (**3**), [$Yb_3(L^{Ph,Ph})_2$(dme)$_2$] (**7**), or [$Yb_5(L^{Ph,Ph})$-(L^1)(L^2)(L^3)(thf)$_4$] (**8**) [L^1 = N($SiMe_3$)C(Ph)CHC(Ph)N($SiMe_2CH_2$), L^2 = NC(Ph)CHC(Ph)H, L^3 = N($SiMe_2CH_2$)] depending on the reaction conditions and stoichiometry. The structures of the crystalline complexes **4,** **6**·2½(hexane), **6**·5(C_6D_6), **7** and **8** have been determined by X-ray crystallography (**1** and **3** have been published).

Introduction

The chemistry of metal β-diketiminates is of substantial current interest.[1] The β-diketiminates have a useful role as *monoanionic* spectator ligands, by virtue of their strong binding to metals, their tuneable and extensive steric demands and the diversity of bonding modes. In some cases, however, the coordinated ligand has been shown to undergo fragmentation, mainly due to deprotonation of one of the substituents on the ligand backbone.[2] For example, in the reaction of [Sc(L^{NN})Cl$_2$] [L^{NN} = {N($CH_2CH_2NEt_2$)C(Me)}$_2$CH] with 2NaN($SiMe_3$)$_2$ deprotonation of one of the β-Me substituents led to the formation of a doubly-methylene-bridged dimer.[2a] Similar Me-deprotonation was also observed in an attempted synthesis of a Ca(Dipp$_2$nacnac)(alkyl) complex [Dipp$_2$nacnac = {N(C_6H_3-Pr$^i_2$-2,6)C(Me)}$_2$CH].[2b] On the other hand, the methyl group of one Pr^i substituent of the Dipp$_2$nacnac ligand was deprotonated in the thermal decomposition of a number of scandium dialkyl complexes [Sc(Dipp$_2$nacnac)(CH_2R)$_2$] (R = H, Ph, Bu^t, $SiMe_3$).[2c] No reduction of the two above-mentioned ligands was observed under rather drastic conditions.[3] Indeed the L^{NN} ligand was used to support a Sc(I) complex,[3a] while the Dipp$_2$nacnac ligand effectively stabilised the mononuclear Al(I) compound [Al(Dipp$_2$nacnac)].[3b]

Another type of bulky β-diketiminato ligand, N($SiMe_3$)C(R)CH-C(R′)N($SiMe_3$)(≡ $L^{R,R'}$), was used in our group for the synthesis of a number of metal complexes, including those of alkali metals, magnesium, aluminium, zirconium, Sn(II), Sn(IV), late transition metals, and the lanthanides.[4] In recent communications we described the reduction of the $L^{R,R'}$ ligand in its Yb complexes with the formation of di- or trianionic β-diketiminates.[5,6] Thus, the synthesis [eqn. (1)] and X-ray structures of the crystalline Yb(II)/($L^{R,R'}$)$^{2-}$ complexes **1** and **2**, their paramagnetism (SQUID, 4–300 K), and solution behaviour [^{1}H/^{1}H NOE (**1**) and ^{6}Li/^{1}H NOE {(**2**) and (**3**)}, Fig. 1 (Ph groups omitted); consistent with the solid state structures], were reported.[5] In a follow-up paper, the synthesis [eqn. (2)] of the trinuclear Yb(II, III)/($L^{R,R'}$)$^-$($L^{R,R'}$)$^{3-}$ complex **3** was described, as was its X-ray structure (outlined in Fig. 2); computational data on model lithiated mono-, di-, and trianionic β-diketiminates were consistent with the structural data and the assignments, with successive one-electron reductions of ($L^{Ph,Ph}$)$^-$ illustrated in Scheme 1.[6] Consistent with this, it is evident that the C–N bond length is a useful marker as to the oxidation state of the ligand; thus reduction of ($L^{Ph,Ph}$)$^-$ (*i.e.*, initially populating the π* CN orbital of $L^{R,R'-}$) lengthens the C–N bond in the di- and trianionic β-diketiminates, and for the latter the alternation of the C–C bond lengths reveals the cross-conjugation. We now report on the synthesis and characterisation of new singly and doubly reduced Li β-diketiminates and further developments arising from novel reductions of [Yb($L^{Ph,Ph}$)$_2$]. Experimental details of the synthesis and characterisation of **3** are also provided.

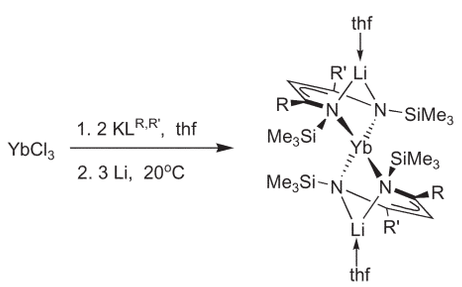

1, R = R' = Ph,
2, R = R' = C_6H_4Ph-4, as 1:1 thf adduct (1)

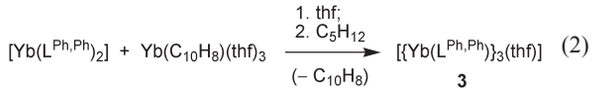

(2)

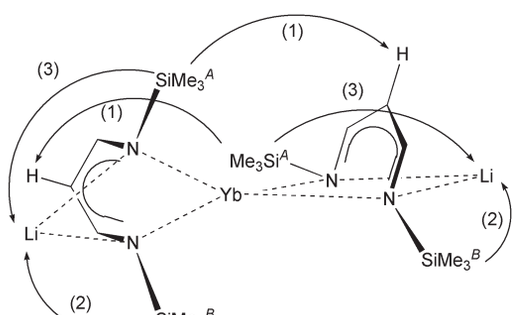

Fig. 1 ^{1}H/^{1}H NOE (1) and ^{6}Li/^{1}H NOE [(2) and (3)] interactions in **1**.[5]

Results and discussion

Reduced homometallic β-diketiminates of lithium

The paramagnetic dilithium compounds [Li(tmen)(μ-$L^{R,R'}$)Li(OEt_2)] (**4**, R = R′ = Ph; or **5**, R = Ph, R′ = Bu^t) and the diamagnetic trilith-

DOI: 10.1039/b405554c

Table 1 Ligand bond lengths (Å) in lithium β-diketiminates. Numbering is shown below, which corresponds to that of **6**

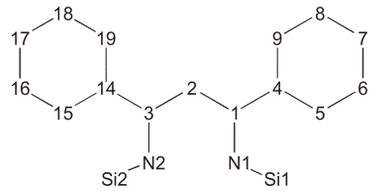

Bond	$[Li(L^{Ph,Ph})]_2$[4b]	**4**	**6**·2½(hexane)[a]	**6**·5(C_6D_6)[a]
N1–C1	1.337(6)	1.390(4)	1.404(5), 1.407(5)	1.415(5), 1.416(5)
N2–C3	1.299(6)	1.386(4)	1.455(4), 1.442(4)	1.447(5), 1.438(5)
C1–C2	1.394(7)	1.418(5)	1.385(5), 1.383(5)	1.370(5), 1.371(5)
C2–C3	1.439(6)	1.418(4)	1.449(5), 1.455(5)	1.458(5), 1.460(5)
C1–C4	1.509(6)	1.480(5)	1.489(5), 1.482(5)	1.498(5), 1.490(5)
C3–C14	1.511(7)	1.483(5)	1.411(5), 1.410(5)	1.406(5), 1.407(5)
N1–Si1	1.747(5)	1.708(3)	1.703(3), 1.700(3)	1.709(3), 1.706(3)
N2–Si2	1.733(5)	1.707(3)	1.691(3), 1.700(3)	1.690(3), 1.687(3)
C4–C5	1.377(7)	1.403(5)	1.401(5), 1.393(6)	1.386(5), 1.390(5)
C5–C6	1.366(7)	1.382(5)	1.385(6), 1.371(6)	1.386(6), 1.379(6)
C6–C7	1.341(7)	1.378(6)	1.389(6), 1.407(6)	1.400(5), 1.405(6)
C7–C8	1.374(7)	1.378(6)	1.397(5), 1.380(6)	1.386(5), 1.388(6)
C8–C9	1.393(7)	1.382(5)	1.389(6), 1.397(5)	1.390(5), 1.392(5)
C9–C4	1.390(7)	1.397(5)	1.387(5), 1.402(5)	1.392(5), 1.398(5)
C14–C15	1.373(7)	1.403(5)	1.445(5), 1.455(5)	1.449(5), 1.455(5)
C15–C16	1.395(7)	1.388(5)	1.395(5), 1.396(5)	1.393(5), 1.387(5)
C16–C17	1.349(7)	1.365(6)	1.413(5), 1.418(5)	1.408(5), 1.406(6)
C17–C18	1.385(7)	1.376(6)	1.405(5), 1.409(5)	1.413(5), 1.410(6)
C18–C19	1.392(7)	1.387(5)	1.382(5), 1.368(5)	1.376(5), 1.384(5)
C19–C14	1.358(7)	1.395(5)	1.459(5), 1.446(5)	1.460(5), 1.456(5)

[a] Value of corresponding bond length of the second ligand is given after comma.

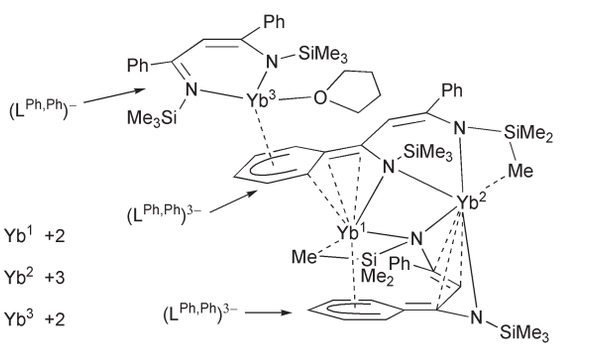

Fig. 2 Schematic representation of the structure of **3** with Yb and ($L^{Ph,Ph}$) charges.[6]

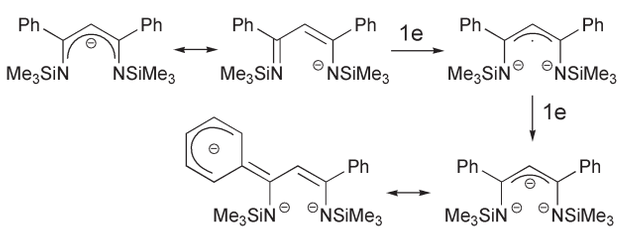

Scheme 1 Successive one-electron reductions: $(L^{R,R'})^- \rightarrow (L^{R,R'})^{2-} \rightarrow (L^{R,R'})^{3-}$.[6]

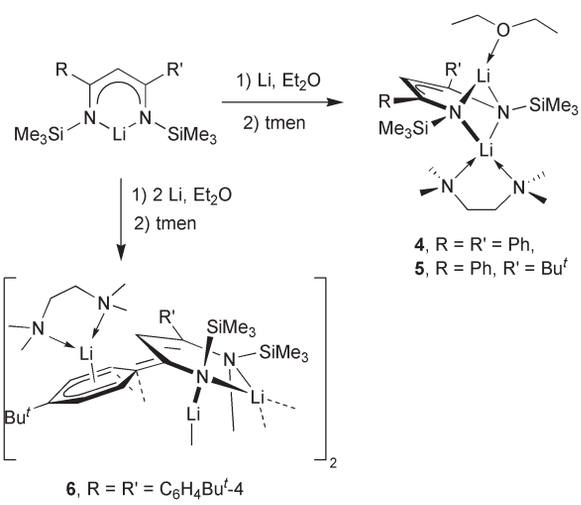

Scheme 2 Synthesis of complexes **4** (dark green), **5** (dark blue) and **6** (dark violet).

ium complex $[Li_3(L^{Ar,Ar})(tmen)]_2$ (**6**, Ar = $C_6H_4Bu^t$-4) were readily obtained by the reduction of the appropriate monolithium β-diketiminate with metallic lithium in the appropriate stoichiometry in diethyl ether, Scheme 2.

The starting complexes were the known $Li(L^{Ph,Ph})$ and $Li(L^{Ph,But})$,[4b] or the newly synthesised $Li(L^{Ar,Ar})$ from $LiCH(SiMe_3)_2$ and 2ArCN. Lithium granules were used in the reductions. The reaction time was shown to depend on the form of the metal. If the metal surface was tarnished, the granules were activated by scratching with a spatula. When the reduction was complete, as evident by the absence of metal, tmen was added, yielding the new crystalline complexes **4, 5**, or **6**, depending on the stoichiometry. In the absence of the neutral co-ligand, the products were powders which were difficult to purify. In contrast, the tmen adducts **4–6** were obtained as well-formed crystals and were easily recrystallised from an appropriate solvent.

The dilithium complexes **4** and **5** were readily soluble in diethyl ether or an arene; EPR spectra of such solutions showed a singlet EPR signal without well defined hyperfine structure; more detailed studies are projected. The ^{1}H-NMR spectra of the complexes in C_6D_6 were not informative. Monitoring the reduction in an NMR tube (in thf-d_8) showed only a very broad signal which shifted from low to high frequency during the course of the reaction.

The molecular structure of the crystalline dilithium complex **4** (Fig. 3 and Table 1) has a puckered Li1N1Li2N2 four-membered ring core, with a 30° torsion angle. The endocyclic angles decrease in the sequence Li2 > Li1 > N2 ≥ N1, and the Li2–N(1 or 2) bonds are shorter than the Li1–N(1 or 2) and by *ca*. 0.05 Å are longer than in the monolithium β-diketiminate $[Li(L^{Ph,Ph})]_2$.[4b] The β-diketiminato ligand both chelates each lithium and bridges the two lithium atoms; Li1 and Li2 are 1.33 Å above and below, respectively, the N1C1C2C3N2 plane.

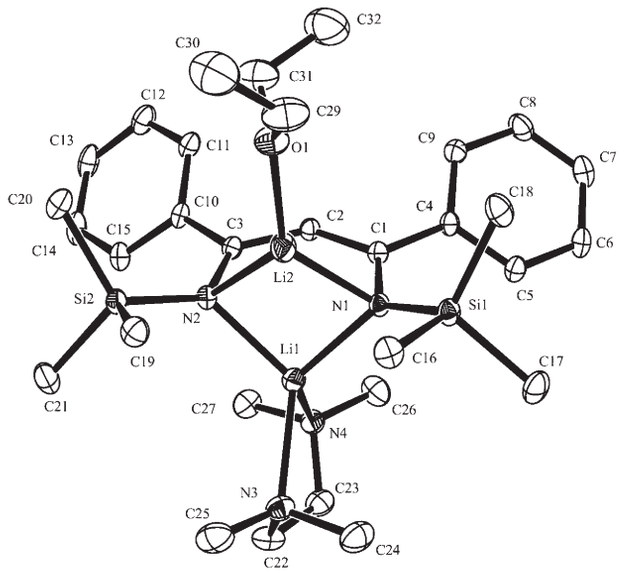

Fig. 3 Molecular structure of [Li(tmen)(μ-$L^{Ph,Ph}$)Li(OEt_2)] (**4**). Selected bond lengths (Å) and angles (°) (see also Table 1): Li1–N1 2.060(6), Li1–N2 2.059(6), Li2–N1 2.008(7), Li2–N2 2.000(7), Li1–C1 2.433(7), Li1–C2 2.540(8), Li1–C3 2.436(7), Li2–C1 2.649(7), Li2–C2 2.815(7), Li2–C3 2.650(7); N1–Li1–N2 92.5(3), Li2–N1–Li1 82.0(3), Li1–N2–Li2 82.3(3), N1–Li2–N2 95.9(3).

The Li1 and Li2 atoms differ in that the former is in a four- and the latter in a three-coordinated environment; this is reflected in the shorter distances to Li2 than Li1 not only from N1 and N2 but also from the C1, C2 and C3 atoms. The endocyclic β-diketiminato bond lengths reveal that there is π-delocalisation in the ligand; this is not extended to the phenyl substituents, the aromatic rings having a *ca*. 36° torsion angle with the N1C1C2C3N2 plane; the Si1 and Si2 atoms are also 0.66 and 0.62 Å, respectively, out of this plane. The ligand geometrical parameters for the crystalline **4** are listed in Table 1, which also shows corresponding data for [Li($L^{Ph,Ph}$)]$_2$[4b] and [Li_3($L^{Ar,Ar}$)(tmen)]$_2$ [**6** as **6**·2½(hexane) and **6**·5(C_6D_6)].

The diamagnetic complex **6** had good solubility and stability in several aprotic solvents. Its multinuclear solution NMR spectra in benzene-d_6 or toluene-d_8 were examined. The ^{1}H-NMR variable temperature spectra of **6** (supported by ^{13}C{^{1}H}- and ^{29}Si{^{1}H}-NMR data) showed that there is an exchange between the two aryl rings. At ambient and higher temperatures the ^{1}H-NMR spectrum showed singlets for both the *tert*-butyl and the trimethylsilyl groups and a broad signal for all the aromatic protons; at 228 K the spectrum revealed singlets for each of the two *tert*-butyl and the two trimethylsilyl groups, two doublets (at δ 7.80 and 7.41) for one of the C_6 ring aromatic protons and four low frequency-shifted (at δ 6.12–5.54) doublets for the other C_6 ring (Fig. 4). These observations are consistent with a low temperature structure in which the negative charge is localised at one of the C_6 rings (Fig. 5). At ambient temperature each C_6 ring alternates in taking part in conjugation with the NC_3N array (Scheme 3). This fluxional process may involve transfer of a lithium atom (Li5 and Li6 in Fig. 5) from one ring to the other.

The ^{6}Li- (Fig. 6) and ^{7}Li-NMR spectra of **6** at low temperature showed four signals consistent with a dimeric "*cis*-like" structure (Fig. 5) having four inequivalent lithium atoms: (i) Li3 and Li4 chelated by the β-diketiminato ligands, (ii) Li5 and Li6 chelated by tmen and η^5-bonded to $C_6H_4Bu^t$, (iii) Li1 bridging the two β-diketiminato ligands and adjacent to the two η^5-$C_6H_4Bu^t$ rings and (iv) Li2 bridging the two β-diketiminato ligands and remote from the two η^5-$C_6H_4Bu^t$ rings.

Upon progressively raising the temperature various ^{7}Li signals sequentially coalesced until at 338 K all signals merged (Table 2). It should be noted that for the Li1 and Li2 signals to merge it is not inevitable that these atoms exchange positions, since the same effect can be achieved as a result of migrating the Li5 and Li6 atoms from one C_6 ring to the other, as shown in Scheme 3. This process seems the more likely, because Li1 and Li2 are more strongly bonded

Table 2 Parameters of multistep dynamic process in complex **3** from VT ^{7}Li-NMR data

Step	Atoms exchanging	T_c/K	$\Delta G^{\ddagger}$/kJ mol^{-1}
1	Li(1) and Li(2)	278	54
2	Li(1, 2) and Li(3, 4)	318	60
3	Li(1, 2, 3, 4) and Li(5, 6)	338	65

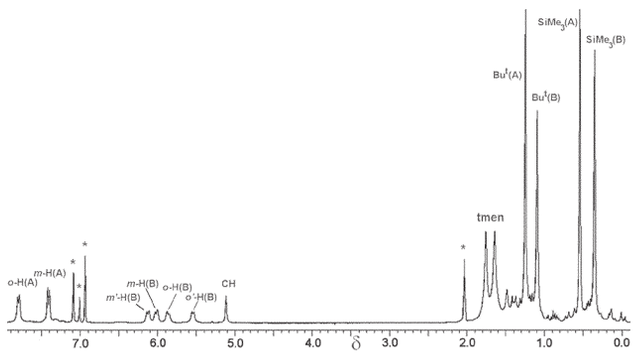

Fig. 4 ^{1}H-NMR spectrum of complex **6** at 228 K (solvent signals are marked with a star). **A** and **B** designate two different sides of the $L^{Ar,Ar}$ ligand as shown in Fig. 5.

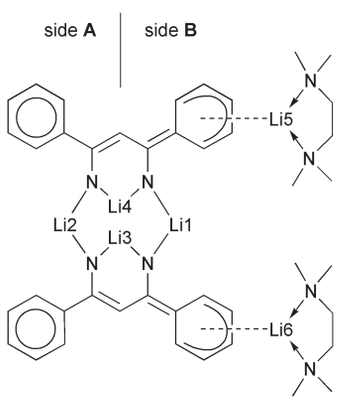

Fig. 5 Schematic representation of lithium positions in a "*cis*-like" isomer of complex **6**. $SiMe_3$ and Bu^t groups are omitted for clarity.

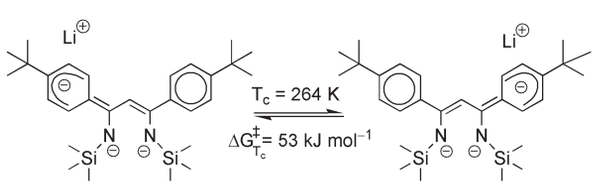

Scheme 3 Dynamic process in solution of complex **6** according to ^{1}H-NMR spectra.

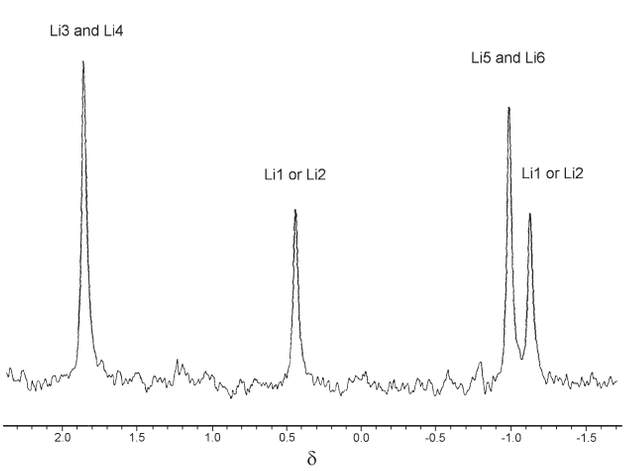

Fig. 6 ^{6}Li-NMR spectrum of complex **6** at 208 K.

between the two ligands whereas Li5 and Li6 can migrate without breaking any Li–N bond. The equality (within the experimental error range) of $\Delta G_{Tc}^{\ddagger}$ for the ^{1}H- and the first ^{7}Li-NMR dynamic processes supports this point of view. The movements of Li5 and Li6 appear to occur simultaneously, because the ^{7}Li-NMR spectra did not reveal a significant presence of a '*trans*-like' isomer.

The two following exchanges (between first the lithium positions Li1/2 and Li3/4 and, finally between Li1/2/3/4 and Li5/6) may involve a dissociation/association sequence of the dimeric structure of **6** and of tmen.

In spite of this multifaceted fluxional behaviour in solution, complex **6** is very robust and can be obtained from different solvents. For example, complex **6** was recovered from an NMR tube after a VT experiment as the crystalline complex **6**·5(C_6D_6).

The molecular structure of crystalline $[Li_3(L^{Ar,Ar})(tmen)]_2$ (**6** as **6**·2½(hexane)) (Fig. 7, Table 1) consists of two β-diketiminato ligands connected to each other by the two lithium atoms Li1 and Li2. Each $L^{Ar,Ar}$ ligand chelates another lithium atom, Li3 or Li4. An additional lithium atom, Li5 or Li6, is connected to one of the aryl rings, with an average Li–C bond length (2.48 Å) similar to that in $[Li(tmen)]_2$(naphthalene) (2.42 Å).[7] Each lithium atom Li5 or Li6 completes its coordination sphere by tmen chelation. Each bridging lithium atom Li1 and Li2 has additional contacts with the carbon atoms of the twisted N1C1C2C3N2 or N3C30C31C32N4 ligand [the angle between the N1C1C2 (or N3C30C31) and C2C3N2 (or C31C32N4) planes is 33° (or 35°)]; in addition, Li1 is close to the *ipso*- and *ortho*-aryl carbon atoms. These carbon atoms are also near to each chelated lithium atom Li3 or Li4. The Li–N bonds form an eight-membered ring core (Fig. 3); the lithium atoms (Li1–Li4) are coplanar with Li···Li′ contacts in the range of 2.66–2.74 Å. The Li–N bond lengths vary from 1.93 to 1.99 Å, and the average Li–N bond length of 1.97 Å is shorter than in **2** (2.03 Å).

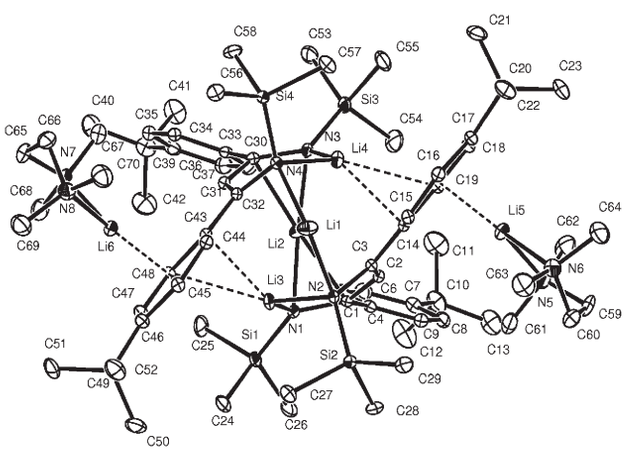

Fig. 7 Molecular structure of $[Li_3(L^{Ar,Ar})(tmen)]_2$ (**6**). Selected bond lengths (Å) and angles (°) for **6**·2½(hexane) [corresponding data for **6**·5(C_6D_6) in parentheses] (see also Table 1): Li(1)–N(2) 1.936(7) [1.990(7)], Li(1)–N(4) 1.930(7) [1.971(7)], Li(2)–N(1) 1.983(7) [1.990(7)], Li(2)–N(3) 1.992(7) [1.979(7)], Li(3)–N(1) 1.991(8) [1.987(8)], Li(3)–N(2) 1.956(6) [1.945(7)], Li(4)–N(3) 1.989(8) [2.005(7)], Li(4)–N(4) 1.954(8) [1.949(7)], Li(5)–Centroid(1) 2.036(7) [1.990(7)], Li(6)–Centroid(2) 2.040(7) [2.005(7)], Li(1)–C(3) 2.430(8) [2.331(7)], Li(1)–C(32) 2.494(7) [2.338(7)], Li(1)–C(15) 2.556(8) [2.336(7)], Li(1)–C(14) 2.600(9) [2.394(7)], Li(1)–C(44) 2.603(9) [2.391(7)], Li(1)–C(43) 2.697(8) [2.432(7)], Li(2)–C(30) 2.118(8) [2.203(7)], Li(2)–C(1) 2.140(8) [2.216(7)], Li(2)–C(31) 2.373(8) [2.448(8)], Li(2)–C(2) 2.471(8) [2.474(8)], Li(3)–C(43) 2.484(8) [2.593(8)], Li(3)–C(48) 2.628(7) [2.519(7)], Li(4)–C(14) 2.543(7) [2.597(7)], Li(4)–C(19) 2.627(7) [2.499(7)]; N(2)–Li(1)–N(4) 131.2(4) [139.8(4)], N(1)–Li(2)–N(3) 176.4(4) [170.8(4)], N(1)–Li(3)–N(2) 105.8(3) [106.8(3)], N(3)–Li(4)–N(4) 106.0(3) [105.7(3)].

The endocyclic β-diketiminato bond lengths (Table 1) reveal substantial bond localisation, with one of the N–C bonds (N1–C1 or N3–C30) shorter than the other (N2–C3 or N4–C32), and one of the C–C bonds (C1–C2 or C30–C31) shorter than the other (C2–C3 or C31–C32). The aryl ring (C14–C19 or C43–C48) is *ca.* 10° out of the plane of the NCC (N2C3C2 or N4C32C31) moiety. In contrast, the other aromatic ring (C4–C9 or C33–C38) is twisted relative to the corresponding CCN (C2C1N1 or C31C30N3) moiety by *ca.* 42°. The exocyclic β-diketiminate C–C bonds to the aryl substituent involved in the conjugation (C3–C14 or C32–C43) are much shorter than those to the other (C1–C4 or C30–C33). The Li-bound C_6 ring has the C–C bond length distribution similar to that in the potassium benzyl $[K(CH_2Ph)(pmdien)]_\infty$,[8] with two elongated C_{ipso}–C_{ortho} bonds (C14–C15 and C14–C19, 1.45 Å) and four "normal" aromatic (av. 1.40 Å) bonds. Each of the other C_6 rings has all six endocyclic bond lengths in the narrow range of 1.38–1.40 Å.

The crystal structure of **6**·5(C_6D_6) shows the same geometric features as described above for **6**·2½(hexane).

Reduced ytterbium β-diketiminates

As previously reported, the heterometallic β-diketiminato complexes of lithium and ytterbium(II) $[Yb\{(\mu\text{-}L^{R,R'})Li(thf)\}_2]$ [R = R′ = Ph (**1**) or R = R′ = C_6H_4Ph-4 (**2**)] were obtained from $YbCl_3$, by reduction of the initially formed corresponding ytterbium(III) β-diketiminate $[Yb(L^{R,R'})_2Cl]$ prepared *in situ*, eqn. (1).[5] Although this method is most convenient, the starting complexes can be isolated before reduction. The mono-β-diketiminato complex of ytterbium(III) $[Yb(L^{Dph,Dph})Cl(\mu\text{-}Cl)_2Li(thf)(OEt_2)]$[9] can be used as a starting material (see Experimental). In contrast, in our hands, use of the new ytterbium(II) precursors $[\{Yb(L^{Ph,Ph})(\mu\text{-}I)(thf)\}_2]$[9] and $[Yb(L^{R,R'})_2]$[4*i*] did not lead to isolation of reduced products.

The outcome of the reductions of $[Yb(L^{Ph,Ph})_2]$ by the ytterbium–naphthalene complex or Yb metal, yielding the crystalline cluster complexes **3**[6] and **7**, or **8**, respectively, is summarised in Scheme 4. Their molecular structures, as revealed by X-ray crystallography, are outlined in Figs. 2 (**3**),[6] 8 (**7**) and 9 (**8**).

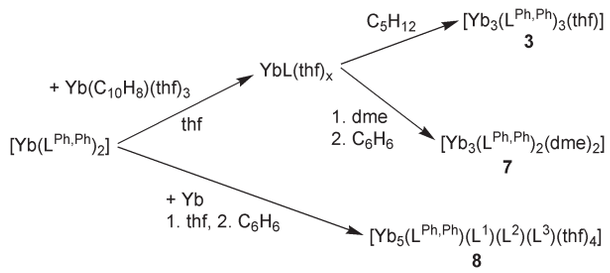

Scheme 4 Reductions of $[Yb(L^{Ph,Ph})_2]$ by Yb or $Yb(C_{10}H_8)(thf)_3$: synthesis of complex **3** (brown),[6] **7** (deep red) and **8** (black) $\{L^1 = L^{Ph,Ph} - H^+$, L^2 = [NC(Ph)CHC(Ph)H] and L^3 = $[N(SiMe_2CH_2)]\}$.

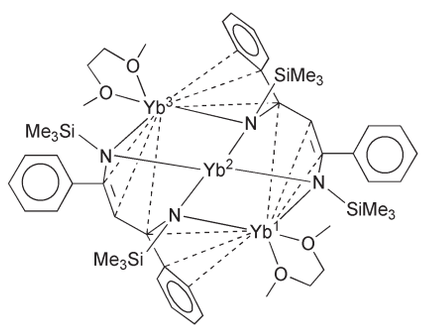

Fig. 8 Schematic representation of the structure of crystalline **7**.

As outlined in the introduction, the reduction of $[Yb(L^{Ph,Ph})_2]$ with $Yb(C_{10}H_8)(thf)_3$ in thf gave the dark brown, crystalline paramagnetic Yb(II)/Yb(III) mixed valence cluster complex **3**.[6] In the course of the reaction a labile dark blue intermediate was initially observed, but upon removing volatiles *in vacuo* **3** was obtained. The ^{1}H-NMR spectrum of the blue solution in thf-d_8 showed one set of signals of a paramagnetically shifted asymmetric β-diketiminate ligand (*i.e.*, showing separate signals for each of the two $SiMe_3$ and two Ph groups), suggesting that the intermediate had a rather simple, apparently monomeric, structure: $(Yb^{+3})(L^{-3})(thf)_x$. Loss of coordinated thf caused aggregation and electron-redistribution resulting in the formation of **3**. In order to stabilise the monomeric species, the chelating solvent 1,2-dimethoxyethane (dme) was

Table 3 Bond lengths (Å) of doubly reduced[a] ligands in ytterbium β-diketiminates.[b] Numbering as in Figs. 10 and 11

Bond		3	7	8
N1–C1	[N3–C22]	1.443(9) [1.456(8)]	1.476(7) [1.471(6)]	1.474(4) [1.464(4)]
N2–C3	[N4–C24]	1.412(8) [1.383(8)]	1.405(6) [1.416(7)]	1.394(4) [1.386(4)]
C1–C2	[C22–C23]	1.475(10) [1.458(9)]	1.471(7) [1.468(7)]	1.478(4) [1.466(4)]
C2–C3	[C23–C24]	1.375(9) [1.367(9)]	1.362(7) [1.364(7)]	1.377(4) [1.380(4)]
C1–C4	[C22–C25]	1.395(9) [1.396(9)]	1.468(7) [1.477(7)]	1.439(4) [1.401(4)]
C3–C10	[C24–C31]	1.487(10) [1.509(9)]	1.484(7) [1.497(7)]	1.492(4) [1.505(5)]
N1–Si1	[N3–Si3]	1.707(5) [1.739(6)]	1.734(4) [1.717(4)]	1.698(3) [1.755(3)]
N2–Si2	[N4–Si4]	1.732(5) [1.720(5)]	1.724(4) [1.718(4)]	1.727(3) [1.721(3)]
C4–C5	[C25–C26]	1.448(10) [1.466(9)]	1.413(8) [1.423(7)]	1.432(5) [1.460(5)]
C5–C6	[C26–C27]	1.385(10) [1.391(9)]	1.376(9) [1.383(8)]	1.367(5) [1.380(5)]
C6–C7	[C27–C28]	1.386(10) [1.382(10)]	1.393(11) [1.400(9)]	1.388(7) [1.413(6)]
C7–C8	[C28–C29]	1.401(11) [1.423(10)]	1.359(11) [1.377(9)]	1.391(7) [1.383(6)]
C8–C9	[C29–C30]	1.386(10) [1.372(9)]	1.397(8) [1.401(8)]	1.392(5) [1.396(5)]
C9–C4	[C30–C25]	1.445(9) [1.459(9)]	1.418(8) [1.415(7)]	1.420(5) [1.459(5)]
C10–C11	[C31–C32]	1.401(12) [1.376(12)]	1.382(8) [1.400(8)]	1.388(5) [1.368(6)]
C11–C12	[C32–C33]	1.411(15) [1.406(13)]	1.395(8) [1.381(8)]	1.382(5) [1.404(6)]
C12–C13	[C33–C34]	1.394(19) [1.33(2)]	1.366(10) [1.389(9)]	1.380(7) [1.361(8)]
C13–C14	[C34–C35]	1.298(17) [1.34(2)]	1.378(11) [1.380(9)]	1.376(7) [1.347(8)]
C14–C15	[C35–C36]	1.381(12) [1.381(16)]	1.378(9) [1.381(8)]	1.395(5) [1.387(6)]
C15–C10	[C36–C31]	1.368(11) [1.373(13)]	1.414(8) [1.390(7)]	1.401(5) [1.389(6)]

[a] The third ligand in **3** is not reduced, its bond lengths are similar to those in $[Li(L^{Ph,Ph})]_2$ (Table 2). [b] Values of corresponding bond length of the second ligand are given in square brackets.

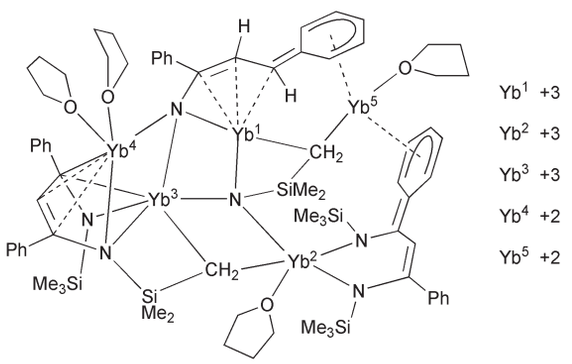

Fig. 9 Schematic representation of the structure of crystalline **8**, with Yb charges.

added to the reaction mixture. The removal of volatiles *in vacuo* was accompanied by a colour change: from blue–violet to red–brown.† Crystallisation from benzene gave deep red crystals of the trinuclear cluster complex $[Yb_3(L^{Ph,Ph})_2(dme)_2]$ (**7**).

Compound **7** was shown (NMR) to be diamagnetic and of better stability and solubility in benzene than **3**, which allowed the assignment of its ^{1}H-NMR spectral signals. As for the spectrum of complex **6**, the ^{1}H-NMR spectrum of **7** in C_6D_6 also showed two sets of signals for the ligand substituents: albeit the signals of the Yb-bound Ph ring aromatic protons (at δ 6.84–6.31) were not significantly shifted to lower frequency. These observations indicate that the $L^{Ph,Ph}$ ligand in **7** is trianionic. In accordance with the solid state structure of **7**, two ^{29}Si- and two ^{171}Yb-NMR signals were observed in toluene/toluene-d_8 solution.

The ease of β-diketiminate reduction was further demonstrated by the reduction of $[Yb(L^{Ph,Ph})_2]$ with Yb metal in thf. The reaction proceeded slowly, with the colour changing successively from green–brown to blue, violet and finally red–brown. Black shiny crystals of complex **8** precipitated in low yield from benzene solution (once crystallised, **8** was no longer soluble in common organic solvents), which were characterised by X-ray diffraction (Fig. 9) as the pentanuclear cluster $[Yb_5(L^{Ph,Ph})(L^1)(L^2)(L^3)(thf)_4]$ [L^1 = $N(SiMe_3)C(Ph)CHC(Ph)N(SiMe_2CH_2)$, L^2 = $NC(Ph)CHC(Ph)H$, L^3 = $N(SiMe_2CH_2)$] containing one doubly reduced β-diketiminato ligand $[L^{Ph,Ph}]^{2-}$, the second (L^1) doubly reduced and deprotonated on one $SiMe_3$ group, and two fragments (L^2 and L^3) of the third ligand as a result of N–Si and N–C bond cleavage. Similar deprotonation of the β-diketiminate–$SiMe_3$ substituent was observed in the attempted synthesis of the Yb(III) tris-β-diketiminate $Yb(L^{Ph,Ph})_3$;[10] $Ln\{N(SiMe_3)_2\}_3$] also underwent such a transformation when treated with an excess of $NaN(SiMe_3)_2$.[11] N–C bond cleavage was observed in another β-diketiminato ligand, $Dipp_2$nacnac, when its Mn(II) complex was treated with Na/K alloy, but only the amido fragment [as $N(H)C_6H_3Pr^i_2$-2,6] was found in the reaction product.[12]

The molecular structures and atom numbering schemes, with selected geometric parameters for complexes **7** and **8** are shown in Figs. 10 and 11, respectively. Comparative data on the bond lengths of the doubly reduced ligands $L^{Ph,Ph}$ in complexes **3, 7** and **8** are given in Table 3.

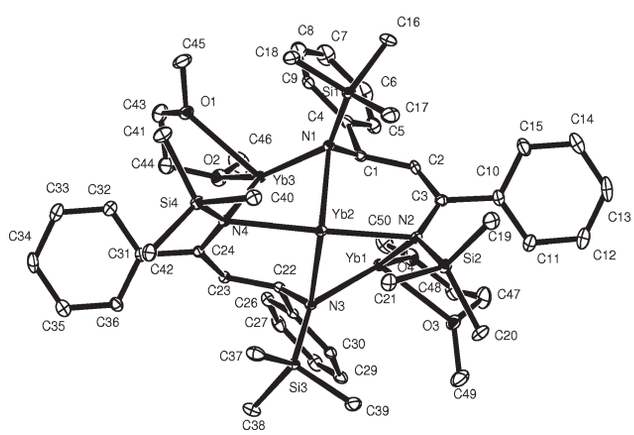

Fig. 10 Molecular structure of $[Yb_3(L^{Ph,Ph})_2(dme)_2]$ (**7**). Selected bond lengths (Å) and angles (°): Yb1–N2 2.526(4), Yb1–N3 2.415(4), Yb1–O3 2.459(4), Yb1–O4 2.585(4), Yb1–C1 2.805(5), Yb1–C2 2.659(5), Yb1–C3 2.670(5), Yb1–C22 2.671(5), Yb1–C25 2.825(5), Yb1–C30 2.851(5), Yb2–N1 2.414(4), Yb2–N2 2.519(4), Yb2–N3 2.397(4), Yb2–N4 2.547(4), Yb3–N1 2.399(4), Yb3–N4 2.495(4), Yb3–O1 2.511(4), Yb3–O2 2.521(4), Yb3–C1 2.673(5), Yb3–C4 2.837(5), Yb3–C9 2.844(5), Yb3–C22 2.816(5), Yb3–C23 2.667(5), Yb3–C24 2.661(5), Yb1–C22–C25 80.3(3), Yb3–C1–C4 80.8(3).

The molecule of complex **3** has the $Yb(L^{Ph,Ph})(THF)$ moiety (see Yb3 in Fig. 2) η^5-coordinated by one of the C_6H_5 rings of the tightly packed $Yb_2(L^{Ph,Ph})_2$ cluster (see Yb1 and Yb2 in Fig. 2). The geometric parameters of the $Yb(L^{Ph,Ph})(THF)$ moiety are very similar to those in the Li and Yb(II) β-diketiminates $[Li(L^{Ph,Ph})]_2$[4b] and $[Yb(L^{Ph,Ph})_2]$,[4i] which suggests that the Yb3 atom is in the +2 oxidation state and the ligand is a "normal" monoanionic β-diketiminate $(L^{Ph,Ph})^-$. Both ligands in the $Yb_2(L^{Ph,Ph})_2$ moiety are bridging and the changes in the C–N and C–C bond lengths, compared to those in $[Li(L^{Ph,Ph})]_2$ (Table 1), indicate that a two-electron reduc-

† If the polar solvent was not removed completely, only non-crystalline products were obtained.

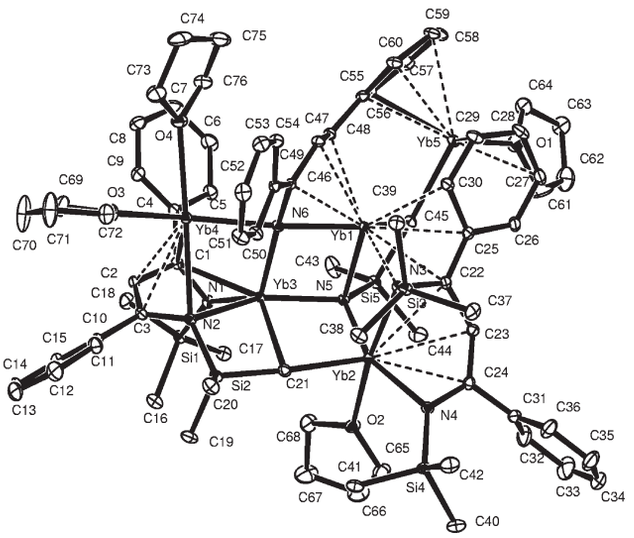

Fig. 11 Molecular structure of complex **8**. Selected bond lengths (Å): Yb1–N5 2.267(2), Yb1–N6 2.334(2), Yb1–N3 2.377(2), Yb1–C45 2.535(3), Yb1–C46 2.582(3), Yb1–C47 2.621(3), Yb1–C48 2.592(3), Yb1–C22 2.716(3), Yb1–C25 2.836(3), Yb1–C30 2.737(3), Yb2–N5 2.184(2), Yb2–N4 2.251(2), Yb2–N3 2.358(2), Yb2–O2 2.384(2), Yb2–C21 2.394(3), Yb2–C24 2.752(3), Yb2–C23 2.839(3), Yb2–C22 2.844(3), Yb3–N1 2.168(3), Yb3–N6 2.174(2), Yb3–N5 2.298(2), Yb3–N2 2.416(3), Yb3–C1 2.570(3), Yb3–C21 2.590(3), Yb4–N6 2.462(2), Yb4–N2 2.577(3), Yb4–O3 2.485(2), Yb4–O4 2.478(2), Yb4–C1 2.679(3), Yb4–C2 2.685(3), Yb4–C3 2.754(3), Yb4–C4 2.951(3), Yb5–O1 2.391(2), Yb5–C45 2.511(3), Yb5–C26 2.989(4), Yb5–C27 2.809(4), Yb5–C28 2.683(4), Yb5–C29 2.725(3), Yb5–C30 2.886(3), Yb5–C55 2.707(3), Yb5–C56 2.790(3), Yb5–C57 2.882(3), Yb5–C58 2.893(3), Yb5–C59 2.856(3), Yb5–C60 2.777(3), Yb3···Yb4 3.17723(18).

tion of $(L^{Ph,Ph})^-$ had occurred with one negative charge delocalised on a C_6H_5 ring (C4–C9 and C25–C30 rings, Table 3). In these two C_6H_5 rings, coordinated to Yb1 and Yb3, the C_{ipso}–C_{ortho} bonds are slightly longer and the exocyclic C_{ipso}–C bonds are shorter than in the $(L^{Ph,Ph})^-$ of $[Li(L^{Ph,Ph})]_2$.[4b] A similar C–C bond length pattern was found in complex **6**. The short Yb2–N bonds and the computational study[6] confirmed that the Yb2 atom is in the +3 oxidation state. The only possible oxidant in these highly reductive reaction conditions is the singly reduced β-diketiminato ligand [*i.e.*, $(L^{Ph,Ph})^{2-}$], which is relatively robust in complexes **4** and **5** with a lithium countercation. In Yb complexes it can either disproportionate into $(L^{Ph,Ph})^{3-}$ and $(L^{Ph,Ph})^-$ (both are present in **3**) or oxidise Yb(II) to Yb(III).

The molecule of complex **7** consists (see Fig. 8) of two very similar (but not crystallographically identical) β-diketiminato ligands and three Yb atoms; each of two of them (Yb1 and Yb3) is η^4-bonded to the endocyclic atoms of one ligand and also η^4-bonded to two endocyclic and two exocyclic (C_{ipso} and C_{ortho}) atoms of the other ligand as well as to the chelating dme molecules; while Yb2, situated above the skeletal atoms of the ligands, is connected only to the N atoms of the β-diketiminates with two close contacts to Me groups of $SiMe_3$ substituents (2.929 and 2.920 Å to C21 and C40, respectively, not shown in Fig. 8). The β-diketiminato skeletal atoms of both ligands are not co-planar: the four atoms C1, C2, C3, N2 connected to the Yb1 atom form one plane (N1 is 1.03 Å out of this plane), while the four atoms N1, C1, C4 and C9 connected to the Yb3 atom form another plane with the dihedral angle of 44.3° between them; a similar arrangement was found in the second ligand. The C–N and C–C bond lengths data (Table 3) support the suggestion that the β-diketiminato ligands in **7** are trianionic with the third negative charge located on C1 (C22 for the second ligand). The C_{ipso}–C_{ortho} bond length elongation of the adjacent Ph ring is not so pronounced as in the complexes **3** and **6**, indicating a smaller extent of negative charge delocalisation in **7**. The Yb3–C1 [2.673(5) Å] and Yb1–C22 [2.671(5) Å] bond lengths may be compared with the Yb–C bond length (2.679 Å) in a closely related complex having an N,C-bonded dianionic ligand [Yb(κ^2-Ph_2CNPh)$(hmpa)_3$].[13] Thus, we conclude that two structurally different types of trianionic β-diketiminato ligands (Fig. 12) are found in its Li and Yb complexes: **C**—with the negative charge delocalised onto one of the Ph substituents and a metal cation η^5- or η^6-coordinated to this Ph ring (complexes **3** and **6**); **D**—with the negative charge largely localised on the β-diketiminate backbone carbon atom and a metal cation interacting only with the C_{ipso} and C_{ortho} of the adjacent Ph ring (complex **7**). Apparently, the geometric constraints of the latter complex prevent the close approach of Yb cations and Ph rings, thus facilitating the **D**-type electron distribution in the ligand.

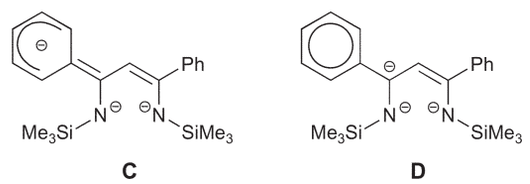

Fig. 12 Negative charge distribution in the two types of β-diketiminato ligand **C** and **D**.

In the molecule of complex **8** (Fig. 9) there are five Yb atoms coordinated by two different β-diketiminato-based ligands: $L^{Ph,Ph}$ and the deprotonated ligand L^1, and two ligand fragments, L^2 [NC(Ph)CHC(Ph)H] and L^3 [$N(SiMe_2CH_2)$]. Bond length data (Table 3) show that L^1 has the **D**-type charge distribution with non-coordinating Ph substituents while $L^{Ph,Ph}$ is of the **C**-type with the negatively charged Ph ring (C25–C30) η^5-bonded to the atom Yb5, which has no Yb–N bond. The ligands L^2 and L^3 are trianionic fragments of a cleaved β-diketiminato ligand: (i) L^2 (Figs. 9 and 13) with a triply-bridging (to Yb1, Yb3 and Yb4) dianionic imido function, the third negative charge being delocalised on the Ph ring (C55–C60) η^6-bonded to the atom Yb5; and (ii) L^3 with a triply-bridging (to Yb1, Yb2 and Yb3) imido function and a bridging (to Yb1 and Yb5) CH_2 group ($^{-2}NSiMe_2CH_2^-$). Imido ligands are quite rare in organolanthanide chemistry; only a few complexes, containing $NSiMe_3$,[14] NPh[15] and $NC_6H_3Pr^i$-2,6[16] ligands have been structurally characterised.

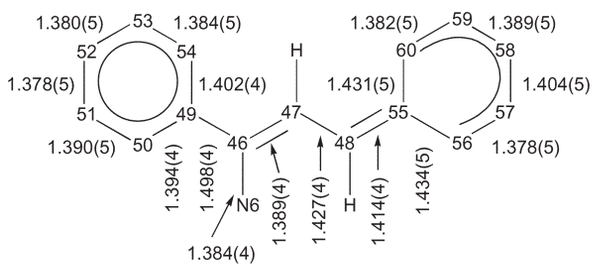

Fig. 13 Bond lengths (Å) in the ligand L^2 of the complex **8**.

The sum of the negative charges on the ligands of complex **8** is −13, which means that three Yb atoms are in the +3 and two Yb atoms are in the +2 oxidation state (3 × 3 + 2 × 2 = 13). Three Yb atoms (Yb1, Yb2 and Yb3) have shorter Yb–N bonds, than Yb(II)–N in $[Yb(L^{Ph,Ph})_2]$,[4i] while the Yb4–N bonds are even longer, suggesting that the Yb1, Yb2 and Yb3 atoms are in the +3 oxidation state with +2 for Yb4. The Yb5 atom has a rather long bond to the bridging CH_2 group [Yb5–C45, 2.511(3) Å], which is similar to the Yb1–C45 and Yb3–C21 bonds but longer than the Yb2–C21 [2.394(3) Å]; the Yb5–C(η^5- and η^6-Ph) bond lengths are similar to Yb(II)–C(η^5-Cp) (2.66–2.78 Å)[17] but significantly longer than the Yb–C bonds in the Yb(III) compound $[YbCp''_2I(thf)]$[18] (2.59–2.69 Å), where the Yb atom is in a similar coordination environment as the Yb5 atom in **8**. We conclude that the Yb5 atom is in the +2 oxidation state.

An unusual feature of complexes **3** and **8** is the presence of a very short contact between the Yb(II) and Yb(III) atoms: 3.275 and 3.177 Å, respectively. The next shortest Yb···Yb contact of 3.301 Å was found in the Yb(III) complex $[\{YbCp(thf)\}_2(Ph_2N_2)_2]$.[19]

Conclusions

In conclusion, we have shown that (i) the β-diketiminato ligand of the type $N(SiMe_3)C(R)CHC(R')N(SiMe_3)$ is readily reduced in its

Li or Yb complexes to a paramagnetic dianion or diamagnetic trianion; (ii) the trianion has two structural types **C** and **D** depending on the negative charge delocalisation and the nature of the metal coordination; and (iii) further reduction of the trianion in its Yb complex leads to ligand fragmentation (C–N and N–Si bond-cleavage and Me group deprotonation) with the formation of new imido ligands.

Experimental

All manipulations were carried out under an inert atmosphere using vacuum/argon line and Schlenk techniques. Solvents were dried and distilled over sodium–potassium alloy (pentane, hexane) or sodium-benzophenone (Et_2O, thf) and stored over a K or Na mirror under argon. Tmen (99%, Acros Organics) was dried and distilled over calcium hydride. $LiCH(SiMe_3)_2$,[20] $Li(L^{Ph,Ph})$,[4b] $Li(L^{Ph,But})$,[4b] and $Yb(L^{Ph,Ph})_2$[4i] were prepared by published procedures. 4-*tert*-Butylbenzonitrile (97%, Aldrich) and lithium (high sodium, granule, 99%, Aldrich) were used without purification. Microanalyses were carried out by Medac Ltd. (Brunel University). The NMR spectra were recorded using the DPX 300 and AMX 500 Bruker instruments and calibrated internally to residual solvent resonances for ^1H and ^{13}C; external $SiMe_4$, LiCl and $[Yb(\eta^5\text{-}C_5Me_5)_2(thf)]$ were used as references for ^{29}Si, ^7Li (and ^6Li) and ^{171}Yb spectra, respectively. All NMR spectra other than ^1H were proton-decoupled and recorded at ambient temperature unless otherwise stated.

Preparations

$Li(L^{Ar,Ar})$

4-*tert*-Butylbenzonitrile (3.46 g, 22.15 mmol) was added to a cooled (0 °C) and stirred solution of $LiCH(SiMe_3)_2$ (1.85 g, 11.12 mmol) in diethyl ether (50 cm^3). The resulting solution was slowly warmed to *ca*. 25 °C and stirred for 2 h. Volatiles were removed *in vacuo* at 70 °C. The product was crystallised from hexane in a freezer at −27 °C yielding yellow crystals of $Li(L^{Ar,Ar})$ (4.35 g, 81%) (Found: C, 71.5; H, 9.21; N, 5.69. $C_{29}H_{45}LiN_2Si_2$: requires C, 71.9; H, 9.36; N, 5.78%). ^1H-NMR (δ, C_6D_6): 7.56 (d, J = 8.35 Hz, *o-H* of $C_6H_4Bu^t$-4, 4 H), 7.24 (d, J = 8.37 Hz, *m-H* of $C_6H_4Bu^t$-4, 4 H), 5.62 (s, C*H*, 1 H), 1.23 (s, Bu^t, 18 H), 0.22 (s, Si*Me*$_3$, 18 H); ^{13}C-NMR (δ, C_6D_6): 175.27 (N*C*($C_6H_4Bu^t$-4)), 150.00 and 147.03 (*ipso*- and *p*-$C_6H_4Bu^t$-4), 127.51 and 124.62 (*o*- and *m*-$C_6H_4Bu^t$-4), 105.66 (*C*H), 34.49 (*C*$(CH_3)_3$), 31.53 (C(*C*$H_3)_3$), 3.28 (Si*Me*$_3$); ^7Li-NMR (δ, C_6D_6): 2.73.

$[Yb\{(\mu\text{-}L^{Ph,Ph})Li(thf)\}_2]$ (1)

Li (0.017 g, 2.50 mmol) was added to a stirred solution of $[Yb(L^{Ph,Ph})_2Cl]$ (0.78 g, 0.83 mmol) in thf (100 cm^3) at *ca*. 20 °C. The dark blue reaction mixture was stirred until the metal had dissolved, then solvent was evaporated and the residue was extracted by pentane (100 cm^3). The extract was concentrated to yield upon cooling dark violet crystals of **1** (0.43 g, 49%). Analytical data of **1** were identical to those published previously.[5]

$[Yb\{(\mu\text{-}L^{Dph,Dph})Li(thf)\}_2]$ (2)

Li (0.010 g, 1.50 mmol) was added to a stirred solution of $[Yb(L^{Dph,Dph})Cl(\mu\text{-}Cl)_2Li(thf)(OEt_2)]$ (0.77 g, 0.74 mmol) in thf (100 cm^3) at *ca*. 20 °C. The dark blue reaction mixture was stirred until the metal had dissolved, then solvent was evaporated and the residue was extracted by ether (100 cm^3). The extract was concentrated to yield upon cooling dark blue crystals of **2**·thf (0.36 g, 67%). Analytical data of **2**·thf were identical to those published previously.[5]

$[Li(tmen)(\mu\text{-}L^{Ph,Ph})Li(OEt_2)]$ (4)

Lithium (0.053 g, 7.64 mmol) was added to a stirred solution of $Li(L^{Ph,Ph})$ (2.82 g, 7.57 mmol) in diethyl ether (100 cm^3) at ambient temperature. The mixture was stirred until the metal had dissolved. Tmen (1.14 cm^3, 7.55 mmol) was added with stirring to the dark green solution, which was concentrated in a vacuum to yield upon cooling dark green crystals of **4** (4.30 g, 74%) (Found: C, 65.1; H, 9.70; N, 9.81. $C_{31}H_{55}Li_2N_4OSi_2$ requires C, 65.3; H, 9.73; N, 9.83%). EPR spectrum (C_6H_6 solution): s, g = 2.0029; (methylcyclohexane solution): s, g = 2.0030.

$[Li(tmen)(\mu\text{-}L^{Ph,But})Li(OEt_2)]$ (5)

Similarly, from Li (0.028 g, 4.03 mmol), $Li(L^{Ph,But})$ (1.40 g, 3.97 mmol) and tmen (0.60 cm^3, 3.97 mmol), dark blue crystals were obtained of **5** (3.52 g, 62%) (Found: C, 63.0; H, 10.79; N, 10.18. $C_{29}H_{59}Li_2N_4OSi_2$ requires C, 63.4; H, 10.82; N, 10.19%). EPR spectrum (diethyl ether solution): s, g = 2.00305.

$[Li_3(L^{Ar,Ar})(tmen)]_2$ (6)

Similarly, from Li (0.072 g, 10.37 mmol), $Li(L^{Ar,Ar})$ (2.49 g, 5.14 mmol) and tmen (0.79 cm^3, 5.21 mmol), after crystallisation from hexane there were obtained dark violet crystals of **6**·2½(hexane), which upon being desolvated in a vacuum (10^{-2} Torr) at room temperature gave **6** (0.76 g, 48%) (Found: C, 67.9; H, 10.07; N, 9.28. $C_{70}H_{122}Li_6N_8Si_4$ requires C, 68.4; H, 10.00; N, 9.11%). ^1H-NMR (δ, C_6D_6): 6.75 (br. s, 8 H; *o*- and *m*-$C_6H_4Bu^t$-4), 5.17 (s, 1 H; C*H*), 1.85 and 1.74 (two br. s, 16 H; tmen), 1.21 (s, 18 H; $C_6H_4Bu^t$-4), 0.44 (s, 18 H; $SiMe_3$); ^1H-NMR (δ, toluene-d_8, 228 K):‡ 7.80 (d, J = 6.58, 2 H; *o*-H of neutral $C_6H_4Bu^t$-4), 7.41 (d, J = 7.85, 2 H; *m*-H of neutral $C_6H_4Bu^t$-4), 6.12 (d, J = 7.89, 1 H; *m′*-H of negatively charged $C_6H_4Bu^t$-4), 6.01 (d, J = 8.50, 1 H; *m*-H of negatively charged $C_6H_4Bu^t$-4), 5.86 (d, J = 8.14, 1 H; *o*-H of negatively charged $C_6H_4Bu^t$-4), 5.54 (d, J = 7.31 Hz, 1 H; *o′*-H of negatively charged $C_6H_4Bu^t$-4), 5.12 (s, 1 H; C*H*), 1.76 and 1.64 (two s, 16 H; tmen), 1.25 (s, 9 H; neutral $C_6H_4Bu^t$-4), 1.09 (s, 9 H; negatively charged $C_6H_4Bu^t$-4), 0.55 (s, 9 H; Si*Me*$_3$ connected to the neutral $C_6H_4Bu^t$-4 side of the ligand), 0.44 (s, 9 H; Si*Me*$_3$ connected to the negatively charged $C_6H_4Bu^t$-4 side of the ligand); ^{13}C-NMR (δ, C_6D_6): 110.92 (s; *C*H), 56 (br. s; *C*H_2, tmen), 46 (br. s; *C*H_3, tmen), 33.59 (s; *C*$(CH_3)_3$), 31.66 (s; C(*C*$H_3)_3$), 5.25 (s; Si*Me*$_3$); ^{29}Si-NMR (δ, C_6D_6, 308 K): −10.08 (s; *Si*Me_3); ^{29}Si-NMR (δ, toluene-d_8, 223 K): −9.25 and −9.63 (two s; *Si*Me_3); ^7Li-NMR (δ, C_6D_6): 1.86 (br. s, Li3 and Li4), −0.21 (br. s, Li1 and Li2), −0.86 (s, Li5 and Li6); ^7Li-NMR (δ, toluene-d_8, 208 K): 1.86 (s, Li3 and Li4), 0.44 (s, Li2 or Li1), −0.95 (s, Li5 and Li6), −1.17 (s, Li1 or Li2); ^6Li-NMR (δ, toluene-d_8, 208 K): 1.85 (s, Li3 and Li4), 0.44 (s, Li2 or Li1), −0.99 (s, Li5 and Li6), −1.13 (s, Li1 or Li2). X-Ray quality crystals of **6**·5(C_6D_6) were isolated from the NMR tube solution of **6**.

$[Yb_3(L^{Ph,Ph})_3(thf)]$ (3)

Solid $Yb(C_{10}H_8)(thf)_3$ (0.120 g, 0.23 mmol) was added to a frozen solution of $[YbL_2]$ (0.189 g, 0.21 mmol) in thf (10 cm^3) and the mixture was warmed up to room temperature with vigorous stirring. Removing the solvent left a deep blue oil, which turned brown while being dried under vacuum. Addition of pentane (10 cm^3) led to crystallisation of the product, which was washed with pentane to remove free naphthalene. X-ray quality crystals of **3** (black needles, 0.045 g, 20%) were obtained from the concentrated pentane extract after it had been stored at 20 °C overnight. Longer storage led to dissolution of the crystals and decomposition of the product. The pentane-washed microcrystalline product was identified as **3** (0.092 g, 41%), on the basis of the strong similarity of its ^1H-NMR spectrum with that of the larger crystals. However, a limited stability and solubility of **3** in C_6D_6 and its paramagnetism prevented further NMR-characterisation.

$[Yb_3(L^{Ph,Ph})_2(dme)_2]\cdot 3(C_6H_6)$ (7)

Solid $Yb(C_{10}H_8)(thf)_3$ (0.233 g, 0.45 mmol) was added to a frozen solution of $[Yb(L^{Ph,Ph})_2]$ (0.199 g, 0.22 mmol) in thf (10 cm^3); dme (2 cm^3) was added by vacuum transfer and the mixture was warmed up to room temperature with vigorous stirring. Removing the sol-

‡ Assignment of the signals was based on selective decoupling at 228 K and NOE experiments at 213 K.

Table 4 Crystal data and structure refinement for **4**, **6**·2½(hexane), **6**·5(C_6D_6), **7** and **8**

Compound	**4**	**6**·2½(hexane)	**6**·5(C_6D_6)	**7**	**8**
Empirical formula	$C_{31}H_{55}Li_2N_4OSi_2$	$C_{70}H_{122}Li_6N_8Si_4{\cdot}2.5(C_6H_{14})$	$C_{70}H_{122}Li_6N_8Si_4{\cdot}5(C_6D_6)$	$C_{50}H_{78}N_4O_4Si_4Yb_2{\cdot}3(C_6H_6)$	$C_{76}H_{109}N_6O_4Si_5Yb_2{\cdot}2.5(C_6H_6)$
Formula weight	569.85	1445.19	1650.3	1664.97	2371.61
Crystal system	Triclinic	Triclinic	Monoclinic	Triclinic	Triclinic
Space group	$P\bar{1}$ (No. 2)	$P\bar{1}$ (No. 2)	$P2_1/n$ (No. 14)	$P\bar{1}$ (No. 2)	$P\bar{1}$ (No. 2)
a/Å	8.7303(3)	12.5155(3)	18.8808(3)	12.2625(1)	14.0487(1)
b/Å	12.4463(4)	18.6263(4)	25.5075(4)	13.0125(1)	18.6777(1)
c/Å	17.1350(8)	22.9370(5)	23.0231(3)	25.652(3)	20.1183(1)
α/°	90.758(1)	112.070(1)	90	78.108(1)	105.265(1)
β/°	100.728(2)	91.730(1)	108.436(1)	82.460(1)	98.119(1)
γ/°	102.226(2)	101.961(1)	90	63.597(1)	110.860(1)
U/Å^3	1785.17(12)	4813.1(2)	10518.9(3)	3583.9(4)	4594.41(5)
Z	2	2	4	2	2
D_c/Mg m^{-3}	1.06	1.00	1.04	1.54	1.71
μ(Mo-Kα)/mm^{-1}	0.13	0.10	0.10	4.00	5.16
Reflections collected	15027	43980	60093	33278	91538
Independent reflections	4869 [R(int) = 0.086]	16340 [R(int) = 0.075]	14168 [R(int) = 0.112]	12426 [R(int) = 0.056]	20911 [R(int) = 0.042]
Reflections with $I > 2\sigma(I)$	3783	12813	9925	10750	18726
Data/restraints/parameters	4869/0/362	16340/114/839	14168/0/1003	12426/0/749	20911/0/1047
Final R indices [$I > 2\sigma(I)$]	$R1$ = 0.065, $wR2$ = 0.139	$R1$ = 0.113, $wR2$ = 0.286	$R1$ = 0.077, $wR2$ = 0.182	$R1$ = 0.035, $wR2$ = 0.084	$R1$ = 0.023, $wR2$ = 0.052
R indices (all data)	$R1$ = 0.091, $wR2$ = 0.153	$R1$ = 0.136, $wR2$ = 0.301	$R1$ = 0.115, $wR2$ = 0.209	$R1$ = 0.045, $wR2$ = 0.089	$R1$ = 0.029, $wR2$ = 0.055

vent yielded a deep violet oil, which turned red–brown upon exposure for 1 h to a dynamic vacuum. Addition of benzene (10 cm^3) gave a dark brown solution, from which X-ray quality crystals of **7** (0.275 g, 75% as black needles, red in thin layer) were formed after storage at room temperature overnight. ^{1}H-NMR (δ, C_6D_6): 7.69 (d, J = 6.9, 2 H, *o*-H of neutral Ph), 7.15–7.09 (overlapped C_6H_6 and *m*- and *p*-H of neutral Ph), 6.84 (t, J = 6.6, 2 H, *m*-H of negatively charged Ph), 6.75 (br. s, 2 H, *o*-H of negatively charged Ph), 6.31 (t, J = 6.6, 1 H, *p*-H of negatively charged Ph), 5.53 (s, 1 H; CH), 2.86 (br. s, 6 H CH_3, dme), 2.61 and 2.29 (two m, AA′BB′, 4 H, dme), 0.52 and 0.49 (two s, 18 H, $SiMe_3$); ^{29}Si-NMR (δ, toluene/toluene-d_8): −3.08 and −13.67 (two s, $SiMe_3$); ^{171}Yb-NMR (δ, toluene/toluene-d_8): 1167 (s, Yb2) and 1107 (s, Yb1 and Yb3).

$[Yb_5(L^{Ph,Ph})(L^1)(L^2)(L^3)(thf)_4]{\cdot}2.5(C_6H_6)$ (8)

Yb metal (0.110 g, 0.64 mmol) was stirred with dry PbI_2 (0.002 g) in thf (10 cm^3) for 1 h, in order to induce activation. [$Yb(L^{Ph,Ph})_2$] (0.262 g, 0.29 mmol) was added, the ampoule was sealed and the reaction mixture was stirred at room temperature for 3 months. Volatiles were removed from the dark red–brown solution *in vacuo* and the residue was extracted with benzene (5 cm^3). Storing the benzene solution for 3 d under ambient conditions produced black shiny crystals of complex **8** (0.020 g, 4% based on $L^{Ph,Ph}$ and its fragments), suitable for X-ray crystallography.

Crystallography

Data for the crystal structure determination of **4, 6**·2½(hexane), **6**·5(C_6D_6), **7** and **8** were collected on a Nonius Kappa CCD diffractometer at 173(2) K with Mo–Kα X-rays (λ = 0.71073 Å). Crystal data and refinement details are listed in Table 4. The structures were solved by a direct method and refined using SHELXL-97.[21] In complex **6**·2½(hexane), there were poorly defined hexane solvate molecules, two in general positions and one on an inversion centre. They were included with a common isotropic displacement parameter, and 1,2 and 1,3 distance constraints. All other non-hydrogen atoms were refined anisotropically; hydrogen atoms were included in riding mode. In complex **8** the hydrogen atoms on C(21) and C(45) (two each); and C(47) and C(48) (one each) were located on a difference map and refined. Other H atoms were riding. One thf ligand and one of the benzene solvate molecules were disordered.

CCDC reference numbers 217238, 223191 and 236144–236146 for compounds **4, 6**·2½(hexane), **6**·5(C_6D_6), **7** and **8**, respectively.

See http://www.rsc.org/suppdata/dt/b4/b405554c/ for crystallographic data in CIF or other electronic format.

Acknowledgements

We thank EPSRC for the award of a fellowship to A. V. K. and to the Royal Society for earlier support and the Leverhulme Trust for grant to A. V. P.

References

1 L. Bourget-Merle, M. F. Lappert and J. R. Severn, *Chem. Rev.*, 2002, **102**, 3031.

2 (*a*) A. M. Neculai, H. W. Roesky, D. Neculai and J. Magull, *Organometallics*, 2001, **20**, 5501; (*b*) S. Harder, *Angew. Chem., Int. Ed. Engl.*, 2003, **42**, 3430; (*c*) P. G. Hayes, W. E. Piers, L. W. M. Lee, L. K. Knight, M. Parvez, M. R. J. Elsegood and W. Clegg, *Organometallics*, 2001, **20**, 2533.

3 (*a*) A. M. Neculai, D. Neculai, H. W. Roesky, J. Magull, M. Baldus, O. Andronesi and M. Jansen, *Organometallics*, 2002, **21**, 2590; A. M. Neculai, C. C. Cummins, D. Neculai, H. W. Roesky, G. Bunkòczi, B. Walford and D. Stalke, *Inorg. Chem.*, 2003, **42**, 8803; (*b*) C. Cui, H. W. Roesky, H.-G. Schmidt, M. Noltemeyer, H. Hao and F. Cimpoesu, *Angew. Chem., Int. Ed. Engl.*, 2000, **39**, 4274.

4 (*a*) P. B. Hitchcock, M. F. Lappert and D.-S. Liu, *J. Chem. Soc., Chem. Commun.*, 1994, 1699; (*b*) P. B. Hitchcock, M. F. Lappert, M. Layh, D.-S. Liu, R. Sablong and S. Tian, *J. Chem. Soc., Dalton Trans.*, 2000, 2301; (*c*) P. B. Hitchcock, M. F. Lappert, D.-S. Liu and R. Sablong, *Chem. Commun.*, 2002, 1920; (*d*) C. F. Caro, P. B. Hitchcock and M. F. Lappert, *Chem. Commun.*, 1999, 1433; (*e*) F. Coslédan, P. B. Hitchcock and

M. F. Lappert, *Chem. Commun.*, 1999, 705; (*f*) P. B. Hitchcock, M. F. Lappert and D.-S. Liu, *Chem. Commun.*, 1994, 2637; (*g*) P. B. Hitchcock, J. Hu, M. F. Lappert, M. Layh, D.-S. Liu, J. R. Severn and S. Tian, *An. Quim. Int. Ed.*, 1996, **92**, 186; (*h*) P. B. Hitchcock, M. F. Lappert and S. Tian, *J. Chem. Soc., Dalton Trans.*, 1997, 1945; (*i*) A. G. Avent, P. B. Hitchcock, A. V. Khvostov, M. F. Lappert and A. V. Protchenko, *J. Chem. Soc., Dalton Trans.*, 2003, 1070.

5 A. G. Avent, A. V. Khvostov, P. B. Hitchcock and M. F. Lappert, *Chem. Commun.*, 2002, 1410.

6 O. Eisenstein, P. B. Hitchcock, A. V. Khvostov, M. F. Lappert, L. Maron, L. Perrin and A. V. Protchenko, *J. Am. Chem. Soc.*, 2003, **125**, 10790.

7 J. J. Brooks, W. Rhine and G. D. Stucky, *J. Am. Chem. Soc.*, 1972, **94**, 7346.

8 D. Hoffmann, W. Bauer, F. Hampel, N. J. R. van Eikema Hommes, P. von R. Schleyer, P. Otto, U. Pieper, D. Stalke, D. S. Wright and R. Snaith, *J. Am. Chem. Soc.*, 1994, **116**, 528.

9 P. B. Hitchcock, A. V. Khvostov and M. F. Lappert, unpublished work.

10 P. B. Hitchcock, M. F. Lappert and A. V. Protchenko, in preparation.

11 M. Karl, K. Harms, G. Seybert, W. Massa, S. Fau, G. Frenking and K. Dehnicke, *Z. Anorg. Allg. Chem.*, 1999, **625**, 2055.

12 J. Chai, H. Zhu, K. Most, H. W. Roesky, D. Vidovic, H.-G. Schmidt and M. Noltemeyer, *Eur. J. Inorg. Chem.*, 2003, **39**, 4332.

13 Y. Makioka, Y. Taniguchi, Y. Fujiwara, K. Takaki, Z. Hou and Y. Wakatsuki, *Organometallics*, 1996, **15**, 5476.

14 M. Karl, G. Seybert, W. Massa, K. Harms, S. Agarwal, R. Maleika, W. Stelter, A. Greiner, W. Heitz, B. Neumüller and K. Dehnicke, *Z. Anorg. Allg. Chem.*, 1999, **625**, 1301.

15 A. A. Trifonov, M. N. Bochkarev, H. Schumann and J. Loebel, *Angew. Chem., Int. Ed. Engl.*, 1991, **30**, 1149.

16 (*a*) J. C. Gordon, G. R. Giesbrecht, D. L. Clark, P. J. Hay, D. W. Keogh, R. Poli, B. L. Scott and J. G. Watkin, *Organometallics*, 2002, **21**, 4726; (*b*) H.-S. Chan, H.-W. Li and Z. Xie, *Chem. Commun.*, 2002, 652.

17 R. D. Rogers, *J. Organomet. Chem.*, 1996, **512**, 97.

18 P. B. Hitchcock, M. F. Lappert and S. Prashar, *J. Organomet. Chem.*, 2000, **613**, 105.

19 W. J. Evans, D. K. Drummond, L. R. Chamberlain, R. J. Doedens, S. G. Bott, H. Zhang and J. L. Atwood, *J. Am. Chem. Soc.*, 1988, **110**, 4983.

20 N. Wiberg and G. Wagner, *Chem. Ber.*, 1986, **119**, 1455.

21 G. M. Sheldrick, *SHELXL-97*, University of Göttingen, Göttingen, Germany, 1997.